

Can KAN Work? Exploring the Potential of Kolmogorov-Arnold Networks in Computer Vision

Yueyang Cang¹ * Yuhang Liu¹ Shi Li¹

¹Tsinghua University
Beijing, China

cangyy23@mails.tsinghua.edu.cn, yh-liu23@mails.tsinghua.edu.cn, shilits@tsinghua.edu.cn

Abstract

Kolmogorov-Arnold Networks (KANs), as a theoretically efficient neural network architecture, have garnered attention for their potential in capturing complex patterns. However, their application in computer vision remains relatively unexplored. This study first analyzes the potential of KAN in computer vision tasks, evaluating the performance of KAN and its convolutional variants in image classification and semantic segmentation. The focus is placed on examining their characteristics across varying data scales and noise levels. Results indicate that while KAN exhibits stronger fitting capabilities, it is highly sensitive to noise, limiting its robustness. To address this challenge, we propose a smoothness regularization method and introduce a Segment Deactivation technique. Both approaches enhance KAN's stability and generalization, demonstrating its potential in handling complex visual data tasks.

1. Introduction

In recent years, neural network[9, 11, 19] architectures have achieved remarkable breakthroughs in computer vision, especially in tasks such as image classification, object detection, and semantic segmentation[17, 22, 23]. Traditional models, particularly Convolutional Neural Networks (CNNs)[10, 13, 17, 18, 28] and the more recent Transformer architectures[4, 4–6, 20, 33–35], have been widely adopted in these areas due to their ability to capture spatial hierarchies and long-range dependencies. CNNs leverage translational invariance through convolutional filters, while Transformers effectively handle complex patterns in images using self-attention mechanisms. These models have thus become mainstream approaches in computer vision tasks.

Alongside these established models, Kolmogorov-Arnold Networks (KANs)[21] have emerged as an intriguing

alternative due to their theoretical efficiency and compact design. KANs are inspired by the Kolmogorov-Arnold representation theorem[14, 15], which suggests that any continuous multivariate function can be represented by a sum of univariate functions. Based on this principle, KANs utilize learnable activation functions, such as B-spline functions[27, 29], allowing them to adapt flexibly to complex patterns with fewer parameters compared to traditional networks. This characteristic makes KANs theoretically appealing for applications where model interpretability and parameter efficiency are prioritized, thus attracting significant research interest[1–3, 8, 32].

This study aims to assess the potential and limitations of KANs in vision tasks by systematically evaluating KANs and their variations across several core computer vision tasks, including image classification, object detection, and semantic segmentation. In our experiments, we examined the response of KAN and Convolutional KAN[1] models under varying data scales and noise levels. The results demonstrate that while KAN and Convolutional KAN exhibit stronger fitting capabilities with larger datasets, their high sensitivity to noise limits their robustness in vision applications.

To enhance KAN stability in vision tasks, we propose a novel smoothness regularization method designed to mitigate excessive oscillations in model parameters. Specifically, this regularization constrains the rate of change in spline functions, ensuring that the KAN model maintains smooth transitions when learning complex patterns, thus enhancing model stability and preventing overfitting. Additionally, we introduce a new technique called Segment Deactivation, which, during training, probabilistically reduces specific spline segments to linear functions. This approach effectively enhances the robustness of the training process by simplifying the model's complexity, leading to improved performance of KANs on high-dimensional vision tasks.

To summarize, our Contributions Are as Follows:

1. Evaluation of KANs in Vision Tasks. We assess

*Corresponding author: Shi Li, shilits@tsinghua.edu.cn

Kolmogorov-Arnold Networks (KANs) across key computer vision tasks, including image classification, object detection, and segmentation, identifying both their strengths and limitations in high-dimensional contexts.

2. Smoothness Regularization. To address KANs' sensitivity to noise, we propose a smoothness regularization method that stabilizes the model, enhancing robustness in noisy environments.

3. Segment Deactivation. We introduce Segment Deactivation, a technique that reduces certain spline segments to linear functions, improving KAN stability and adaptability to vision tasks.

2. Related Work

Kolmogorov-Arnold representation theorem

The Kolmogorov-Arnold representation theorem, proposed by mathematicians Andrey Kolmogorov and Vladimir Arnold, states that any continuous multivariate function $f(x)$ can be represented as a sum of specific types of series, known as Kolmogorov series, composed of univariate continuous functions. For a continuous function $f : [0, 1]^d \rightarrow \mathbb{R}$, the theorem allows it to be decomposed into a finite combination of univariate functions as follows:

$$f(x_1, \dots, x_d) = \sum_{q=1}^{2d+1} \Phi_q \left(\sum_{p=1}^d \varphi_{q,p}(x_p) \right) \quad (1)$$

where Φ_q and $\varphi_{q,p}$ are continuous univariate functions. The importance of the Kolmogorov-Arnold representation theorem lies in its demonstration that any multivariate continuous function can be represented by a finite combination of univariate functions, significantly simplifying the representation and computation of complex functions. This property provides theoretical support for high-dimensional data modeling and has inspired neural network architectures, especially in the areas of function approximation and dimensionality reduction.

Kolmogorov-Arnold Networks

Kolmogorov-Arnold Networks (KAN) are a neural network architecture inspired by the Kolmogorov-Arnold representation theorem. KAN approximates multivariate functions by decomposing them into combinations of univariate transformations and linear mappings. Specifically, KAN employs nonlinear spline-based activation functions, such as B-splines, to approximate complex functions with high-dimensional data inputs effectively. KAN has demonstrated promising results in function approximation and high-dimensional data modeling, leveraging its capacity for powerful, flexible function representation.

Convolutional KAN

Convolutional KAN (CKAN) was introduced shortly after the development of Kolmogorov-Arnold Networks (KAN) to enhance their performance in visual tasks. By incorporating convolutional layers, CKAN combines the spatial feature extraction capabilities of Convolutional Neural Networks (CNNs) with the nonlinear approximation power of KAN's spline-based activation functions. In CKAN, the integration of KAN within convolutional layers enables the model to effectively capture spatial hierarchies in images while leveraging the expressive power of spline functions for complex nonlinear transformations. This approach allows CKAN to perform well in various vision tasks by unifying the advantages of CNNs in local feature extraction with KAN's advanced representational flexibility.

3. Method

3.1. Kolmogorov-Arnold Networks (KAN)

Kolmogorov-Arnold Networks (KAN) are neural architectures derived from the Kolmogorov-Arnold representation theorem, which establishes that any continuous multivariate function can be represented by a sum of univariate functions. Leveraging this theorem, KAN decomposes high-dimensional inputs into univariate transformations, allowing effective approximation of complex multivariate functions.

Given an input vector $\mathbf{x} = (x_1, x_2, \dots, x_{d_{\text{in}}})$ with dimension d_{in} , KAN models the function $f : \mathbb{R}^{d_{\text{in}}} \rightarrow \mathbb{R}^{d_{\text{out}}}$ as follows:

$$f(\mathbf{x}) = \Phi \circ \mathbf{x} = \left[\sum_{i=1}^{d_{\text{in}}} \varphi_{i,1}(x_i), \dots, \sum_{i=1}^{d_{\text{in}}} \varphi_{i,d_{\text{out}}}(x_i) \right] \quad (2)$$

where each $\varphi_{i,j}$ represents a univariate transformation on input component x_i , and Φ encapsulates the composite mapping applied across input dimensions. KAN typically utilizes **B-spline functions** as activation functions due to their flexibility and smoothness, providing an enhanced capacity to capture nonlinearity.

The process of function approximation in KAN consists of several key steps:

1. **Univariate Transformations:** Each input x_p undergoes transformation through a univariate function $\varphi_{q,p}(x_p)$, producing intermediate values h_q :

$$h_q = \sum_{p=1}^d \varphi_{q,p}(x_p) \quad (3)$$

2. **Nonlinear Activation with B-splines:** Each summation result h_q is then passed through a nonlinear activation,

formulated as a combination of the **SiLU (Sigmoid Linear Unit)** and a B-spline function:

$$h'_q = \phi_q(h_q) = w_b \cdot \text{silu}(h_q) + w_s \cdot \text{spline}(h_q) \quad (4)$$

where $\text{silu}(x) = \frac{x}{1+e^{-x}}$ and $\text{spline}(x) = \sum_i c_i B_i(x)$, with $B_i(x)$ as the basis functions of the B-spline.

3. **Final Output Computation:** The network aggregates the transformed hidden layer outputs to yield the final function approximation:

$$y = \sum_{q=1}^{2d+1} \phi_q \left(\sum_{p=1}^d \varphi_{q,p}(x_p) \right) \quad (5)$$

This architecture effectively represents high-dimensional functions by leveraging the spline-based transformations, with SiLU and B-spline activations ensuring smooth, nonlinear responses. The univariate mapping strategy aligns with the Kolmogorov-Arnold theorem, enabling KAN to achieve accurate approximations for complex function classes.

3.2. Convolutional KAN (CKAN)

Convolutional Kolmogorov-Arnold Networks (CKAN) extend KAN by embedding its spline-based transformations into convolutional architectures, thus enhancing the network's suitability for visual tasks involving spatially structured data. CKAN fuses convolutional operations with KAN's expressive activation, optimizing it for capturing local image structures and complex non-linear interactions.

The specific architecture of CKAN is as follows:

1. **Convolutional Transformation:** The network begins with convolutional layers, which perform spatial filtering on the input data. For each input feature map \mathbf{x}_i , the convolutional output \mathbf{y}_i is computed as:

$$\mathbf{y}_i = \sum_j \mathbf{W}_j * \mathbf{x}_i + b_i \quad (6)$$

where \mathbf{W}_j are the learnable convolutional kernels, $*$ denotes the convolution operation, and b_i is a bias term. This process generates feature maps capturing spatial hierarchies in the data, which are essential for modeling visual patterns and textures.

2. **KAN-based Activation with Splines:** After convolution, each feature map \mathbf{y}_i is passed through an activation function defined by univariate spline transformations. This is formulated as:

$$\mathbf{z}_i = \sum_k w_k \phi_k(\mathbf{y}_i) \quad (7)$$

where $\phi_k(\mathbf{y}_i)$ are the spline-based activation functions applied to each convolved feature map, and w_k are the weights applied to each spline function.

The spline functions in KAN are leveraged to achieve high non-linear representation, allowing CKAN to capture intricate dependencies and variations within local image features.

CKAN integrates KAN's nonlinear activation into convolutional processing, optimizing it for high-dimensional visual data with structured spatial dependencies. By coupling CNN's spatial pattern extraction with KAN's advanced spline-based nonlinearity, CKAN provides an expressive architecture for complex computer vision tasks.

3.3. The Potential of KAN in Computer Vision

As illustrated in Figure 1, we present a simple edge detection example to demonstrate the potential of KAN in computer vision tasks. This example highlights the difference between KAN and a traditional MLP [25] in identifying specific edge patterns within an image.

In this scenario, the goal is to detect left and right edges within a set of pixels. For simplicity, we use a 4-pixel configuration, where the left edge is defined by a transition from a black (value of 1) to a white (value of 0) pixel, while the right edge shows the opposite transition, from white (value of 0) to black (value of 1).

In this example:

- **Left Edge Detection with MLP:** An MLP with a single hidden layer can easily identify the left edge, as shown by the binary matrix in the upper half of the figure. Using a straightforward linear combination of the pixel values with specific weights and a bias term, the MLP correctly classifies the left edge.
- **Right Edge Detection with KAN:** When detecting the right edge pattern, however, an MLP struggles because of its linear structure, which lacks the necessary nonlinearity. By contrast, KAN, with its spline-based representation, can capture this pattern by adjusting segment parameters dynamically, enabling it to distinguish between subtle differences in pixel arrangements. As shown in the lower half of the figure, KAN accurately identifies the right edge due to its ability to fit more complex functions, making it better suited for this type of task.

This example illustrates that while MLPs are effective for simpler patterns, KAN's nonlinear fitting ability allows it to capture more intricate visual features, such as edges of varying orientations or structures within an image. This capability is particularly valuable in computer vision, where data often contains complex spatial relationships, edges, and boundaries that require robust modeling beyond linear transformations.

By adapting to local patterns within an image, KAN demonstrates the potential to improve tasks like edge detection, object recognition, and segmentation. These initial results suggest that KAN, with proper regularization and techniques like Segment Deactivation to enhance gen-

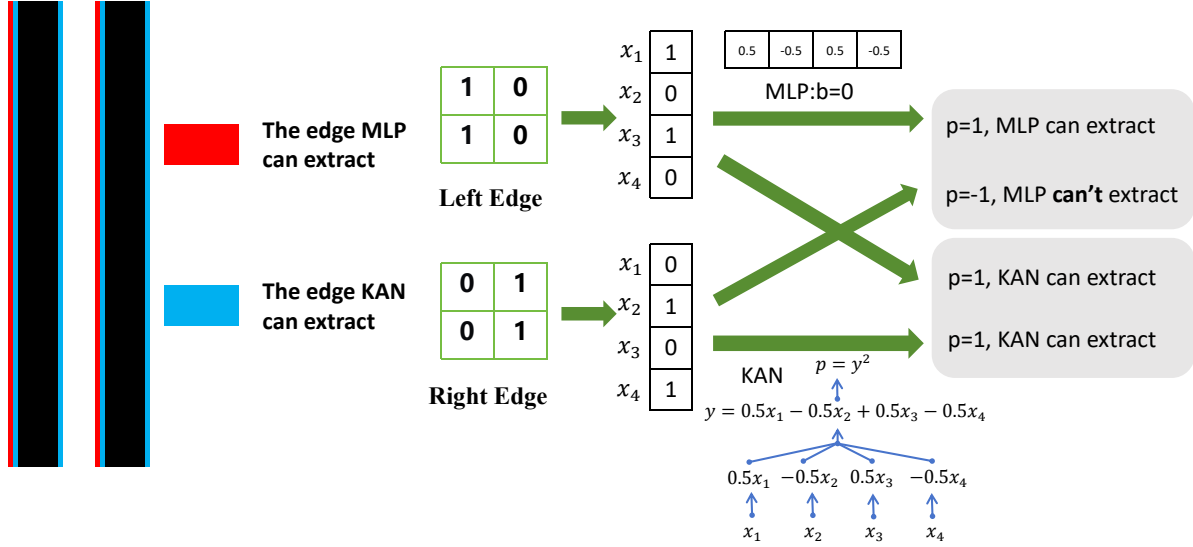


Figure 1. **Illustration of KAN’s Potential in Edge Detection.** This figure presents an example comparing the edge detection capabilities of KAN and a traditional MLP. The MLP successfully detects the left edge pattern but struggles with the right edge, while KAN accurately identifies both patterns due to its nonlinear fitting capacity.

eralization, could serve as a powerful tool in visual pattern recognition, leveraging its fitting strength to handle complex visual structures while minimizing sensitivity to noise.

4. Experiments

In this section, we present a series of experiments designed to evaluate the performance of Kolmogorov-Arnold Networks (KAN) and Convolutional KAN (CKAN) across several core computer vision tasks. These preliminary experiments help us assess the strengths and limitations of KAN in visual pattern recognition, providing a foundation for more in-depth analysis. Specifically, we apply KAN and CKAN to image classification and semantic segmentation tasks, using three widely-used datasets: CIFAR-10 [16], CIFAR-100 [16], and PASCAL VOC2012 [7]. Our goal is to provide a representative evaluation of KAN’s capabilities and limitations in computer vision through comprehensive experimentation. Subsequently, we will conduct an in-depth analysis and discussion based on the experimental results and consider potential ways to improve KAN’s performance in computer vision tasks.

4.1. Experiment 0: Preliminary Evaluation of KAN and CKAN on Core Vision Tasks

Image Classification. We selected the CIFAR-100 dataset to conduct a preliminary experiment. MobileNetV2[12, 26] was used as the baseline model, and we performed two replacement experiments: first, by substituting the final MLP layer with KAN for classification, and second, by replacing either the first or the final CNN layer in MobileNetV2 with CKAN. Due to the high memory requirements of CKAN, we limited our experiments to replacing only a single layer. To ensure a direct comparison between KAN and MLP, as well as CKAN and CNN, we used a minimal training configuration without any image augmentation or regularization techniques, employing cross-entropy as the loss function.

Semantic Segmentation. We selected the PASCAL VOC2012 dataset for our experiments, using UNet[24] as the baseline model. Since UNet does not include an MLP, we only replaced the final CNN layer used for classification with CKAN to conduct the experiment. Similarly, we adopted the simplest training configuration for this experiment. For all replacements in these experiments, we set the grid size to 5 and the spline order to 3.

Result. As shown in Table 1, the experimental results in-

dictate that the performance of models incorporating KAN and CKAN in classification and segmentation tasks is generally lower than that of the baseline models. This result is unexpected, as the nonlinear characteristics of KAN and CKAN could theoretically enhance the model’s fitting capability. This observation motivates further investigation into why the nonlinear fitting abilities of KAN and CKAN have not been fully leveraged in computer vision tasks.

4.2. Experiment 1: Effect of Dataset Size on KAN Performance

Setup. In the following experiments, we designed three model architectures to evaluate the performance and potential of KAN and CKAN in visual tasks. First, we used a standard CNN model (CNN+MLP) as the baseline, which includes two convolutional layers followed by an MLP for classification. We then constructed two alternative models: one that replaces the first convolutional layer with CKAN (CNN+CKAN+MLP) and another that replaces the final MLP with KAN (CNN+KAN). The detailed configurations of these three models are shown in Table 2.

To verify whether KAN and CKAN indeed possess superior fitting capabilities, we designed the following experiments. Theoretically, KAN’s nonlinear spline functions should provide a fitting advantage over linear functions, although this was not clearly evident in the initial experiment. To further investigate, we conducted a series of experiments on CIFAR-10 using varying dataset sizes, ranging from 20% to 100% (20%, 40%, 60%, 80%, 100%) of the available training data. In these experiments, we ensured balanced class distribution, with an equal number of samples from each class at every dataset size.

Results. As shown in Table 3, CNN + KAN consistently outperformed the baseline CNN + MLP across all dataset sizes, demonstrating the stable fitting capability of KAN. CKAN + CNN + MLP, however, only surpassed the baseline at the 100% dataset size, indicating that CKAN’s fitting ability becomes more evident with larger data volumes. These findings reveal that both KAN and CKAN possess stronger nonlinear fitting capabilities compared to the baseline. However, as model complexity and dataset size increase, their fitting potential can be more fully realized. This experiment validates the enhanced capacity of KAN and CKAN to capture complex patterns, especially with sufficient data.

4.3. Experiment 2: Robustness of KAN and CKAN to Label Noise

In Experiment 1, we observed that both KAN and CKAN exhibit strong fitting capabilities. However, theoretically, CKAN should have a superior fitting ability compared to KAN. Nevertheless, in our experimental results, CKAN’s performance was less than satisfactory. We hypothesize that

this may be due to the higher complexity of input in vision tasks, which are more likely to include noise and outliers. This increased fitting capacity may, therefore, lead to lower accuracy on the test set. To investigate this, we designed Experiment 2, where we intentionally introduce label noise to evaluate the performance of CKAN and KAN in noisy environments, aiming to assess their robustness against noise in vision tasks.

Setup. In Experiment 2, we evaluated the robustness of different model architectures under varying levels of label noise. We gradually increased the noise from 10% to 50% and observed the impact on model performance. The three models tested were CNN as the baseline, CKAN+CNN+MLP with CKAN replacing the first convolutional layer, and CNN+KAN with KAN replacing the final MLP layer.

Results. As shown in Table 4, the accuracy of all models decreases as noise levels increase, with CKAN+CNN+MLP and CNN+KAN experiencing a more pronounced decline compared to the baseline CNN model. Although the initial performance of KAN and CKAN models is slightly better than the baseline under low noise conditions, they exhibit greater sensitivity to noise at higher noise levels. This suggests that, despite the strong fitting capabilities of KAN and CKAN, these abilities may lead to overfitting when noise is introduced, thus reducing their robustness in noisy environments.

4.4. Experiment 3: Impact of Regularization on the Generalization of KAN and CKAN

In Experiment 2, we observed that noise significantly impacts the performance of KAN and CKAN models. Based on this finding, Experiment 3 aims to study the effect of regularization on the generalization ability of KAN and CKAN. We introduced L1 regularization [31] in the models and tested various regularization parameters to observe its influence on performance in visual tasks. This experiment evaluates whether regularization can effectively enhance the stability and robustness of KAN and CKAN models.

Setup. To investigate the impact of L1 regularization on the generalization ability of KAN and CKAN, we conducted two experiments with different data conditions:

- **Noisy Environment.** We applied four L1 regularization strengths (0, 0.0001, 0.001, 0.01) on a dataset with 30% label noise.
- **Normal Environment with Limited Data.** We repeated the experiment on a clean 60% subset of the dataset, testing the same regularization strengths.

Results. As shown in Tables 5 and 6, we observed that with moderate L1 regularization, models incorporating KAN and CKAN surpassed the baseline CNN model in accuracy. This suggests that KAN and CKAN’s fitting capabilities were better utilized without being overly affected

Task	Model	Replacement	Accuracy / mIoU (%)
Image Classification	MobileNet	Baseline	61.14
	MobileNet	KAN (MLP replaced)	60.98
	MobileNet	First Layer CKAN	59.76
	MobileNet	Last Layer CKAN	60.29
Semantic Segmentation	UNet	Baseline	63.28
	UNet	CKAN (Final CNN replaced)	62.13

Table 1. **Performance Comparison of Baseline Models with KAN and CKAN on CIFAR-100 and PASCAL VOC2012.**

Model	First Layer	Second Layer	Final Layer
CNN+MLP	CNN (3→32, 3x3)	CNN (32→64, 3x3)	MLP
CNN+CKAN+MLP	CKAN (3→32, 3x3)	CNN (32→64, 3x3)	MLP
CNN+KAN	CNN (3→32, 3x3)	CNN (32→64, 3x3)	KAN

Table 2. **Experimental Model Configurations.** The baseline model (CNN+MLP) serves as a control for comparison with the CKAN and KAN-modified models.

Model	20%	40%	60%	80%	100%
CNN+MLP	62.31%	67.26%	69.93%	71.33%	71.96%
CKAN+CNN+MLP	61.82%	67.05%	69.03%	70.91%	72.44%
CNN+KAN	64.02%	68.15%	70.41%	72.13%	72.58%

Table 3. **Performance of Different Models on CIFAR-10 with Varying Dataset Sizes.** Each column shows the accuracy (%) of each model as the dataset size increases from 20% to 100%.

Model	10%	20%	30%	40%	50%
CNN+MLP	69.13%	67.93%	65.38%	63.88%	62.87%
CKAN+CNN+MLP	69.59%	66.73%	64.19%	62.56%	58.43%
CNN+KAN	69.95%	67.81%	64.33%	62.84%	59.20%

Table 4. **Performance of Different Models with Increasing Label Noise.** Each column represents the accuracy (%) as the label noise increases from 10% to 50%.

by noise points and outliers, highlighting the importance of regularization for enhancing their generalization. Additionally, we observed that while CKAN demonstrated strong fitting ability, its performance was generally inferior to that of KAN, with CKAN also requiring more memory and being computationally slower. Based on these findings, we focus on KAN in the next experiments to further explore its potential.

4.5. Experiment 4: Enhanced Regularization and Segment Deactivation for Improved KAN Generalization

Based on the results of Experiment 3, we found that improving the generalization ability of KAN and reducing its sensitivity to noise is crucial. To address this, we propose Smoothness Regularization method and introduce the Segment Deactivation technique, aiming to enhance the robustness and generalization of KAN.

Smoothness Regularization Method. To enhance the

generalization ability of KAN and reduce its sensitivity to noise, we introduce a smoothness regularization method tailored to KAN’s spline-based structure. Specifically, this regularization penalizes abrupt changes in the spline’s behavior, encouraging smooth transitions between segments and preventing overfitting to noisy data. The smoothness regularization term is formulated as follows:

$$\mathcal{R}_{\text{smooth}} = \lambda \sum_{i=1}^N \int \left(\frac{d^2 S_i(x)}{dx^2} \right)^2 dx, \quad (8)$$

where $S_i(x)$ is the spline function for segment i , N is the total number of spline segments, and λ is the regularization strength. This term penalizes the second derivative of each spline segment, promoting a smoother overall function.

This smoothness regularization leverages KAN’s spline-based structure, improving its stability across segments while maintaining strong fitting capability and mitigating the impact of noise.

Model	0	0.0001	0.001	0.01
CNN+MLP	65.38%	65.54%	65.79%	63.47%
CKAN+CNN+MLP	64.19%	64.98%	65.94%	63.02%
CNN+KAN	64.33%	65.26%	66.03%	63.94%

Table 5. **Effect of L1 Regularization on Model Accuracy with 30% Label Noise.** Each column shows the accuracy (%) of each model with increasing L1 regularization values.

Model	0	0.0001	0.001	0.01
CNN+MLP	69.93%	70.01%	70.23%	67.58%
CKAN+CNN+MLP	69.03%	69.98%	70.36%	67.32%
CNN+KAN	70.41%	70.98%	71.56%	63.94%

Table 6. **Effect of L1 Regularization on Model Accuracy with 60% Dataset Size.** Each column shows the accuracy (%) of each model with increasing L1 regularization values.

Segment Deactivation Technique. The Figure To further improve the robustness and generalization of KAN, we propose a novel regularization technique termed *Segment Deactivation*. Similar to Dropout [30], this approach selectively deactivates specific spline functions, reducing them to linear functions with a certain probability only during the training phase. By simplifying the entire spline function into a straight line in selected cases, Segment Deactivation helps prevent overfitting and mitigates sensitivity to noise. During testing, all spline functions operate in their original nonlinear form, allowing the model to perform with its full fitting capacity.

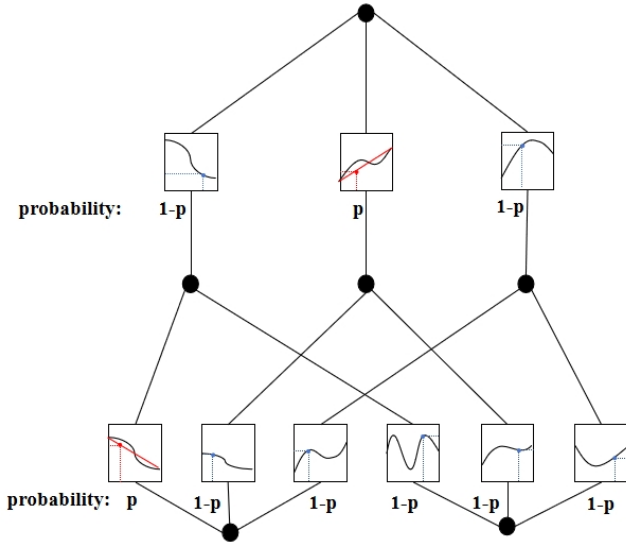


Figure 2. **Illustration of Segment Deactivation Technique.** This figure demonstrates the simplification process where the entire spline function between its start and end points is replaced with a linear connection (shown in red) with a certain probability p . This technique reduces complexity in noisy segments, enhancing generalization.

The Segment Deactivation regularization is implemented as follows:

$$S(x) = \begin{cases} S(x) & \text{with probability } 1 - p, \\ a \cdot x + b & \text{with probability } p, \end{cases} \quad (9)$$

where $S(x)$ is the original spline function for a specific input, and a and b are coefficients that define a line connecting the start and end points of the entire spline function. The probability p controls the likelihood of deactivation, balancing between preserving the spline’s expressiveness and encouraging generalization. The simplified Segment Deactivation Technique process is illustrated in Figure 2.

By introducing controlled linearity over the entire spline function, Segment Deactivation reduces the risk of overfitting to noise and enhances KAN’s generalization capability. This technique is particularly beneficial in noisy environments, as it forces the model to learn more generalized patterns across the data.

We conducted experiments on both CIFAR-10 and CIFAR-100 datasets to evaluate the effectiveness of the proposed Smoothness Regularization method and Segment Deactivation technique in improving the generalization of KAN. For each dataset, we tested four configurations: KAN alone, KAN with Smoothness Regularization, KAN with Segment Deactivation, and KAN with both techniques combined. This ablation study allows us to examine the individual and combined contributions of each method to the model’s accuracy.

Results. As shown in Tables 7 and 8, both the Smoothness Regularization method and Segment Deactivation technique resulted in notable accuracy improvements when added to the KAN-enhanced models on both CIFAR-10 and CIFAR-100. In particular, the configuration combining both methods achieved the highest accuracy, demonstrating that the proposed techniques effectively mitigate overfitting and improve generalization. Furthermore, these results indicate that each method contributes positively to

Model Configuration	Accuracy (%)
CNN + MLP	71.96
CNN + KAN	72.58
CNN + KAN + Smoothness Regularization Method	73.04
CNN + KAN + Segment Deactivation Technique	73.12
CNN + KAN + Smoothness Regularization Method + Segment Deactivation Technique	73.30

Table 7. **Performance Comparison of CNN with KAN, Smoothness Regularization, and Segment Deactivation Techniques on CIFAR-10 Dataset.** Each row shows the accuracy (%) for different configurations of CNN with the proposed methods on CIFAR-10.

Model Configuration	Accuracy (%)
MobileNet	61.14
MobileNet + KAN	60.98
MobileNet + KAN + Smoothness Regularization Method	62.03
MobileNet + KAN + Segment Deactivation Technique	62.37
MobileNet + KAN + Smoothness Regularization Method + Segment Deactivation Technique	62.98

Table 8. **Performance Comparison of MobileNet with KAN, Smoothness Regularization, and Segment Deactivation Techniques on CIFAR-100 Dataset.** Each row shows the accuracy (%) for different configurations of MobileNet with the proposed methods on CIFAR-100.

KAN’s robustness, and when used together, they complement each other to further enhance performance.

5. Conclusions

This study explores the potential of Kolmogorov-Arnold Networks (KAN) in computer vision tasks. Despite KAN’s strong fitting capability, our experimental results indicate that the high complexity of visual data and the prevalence of noise present significant challenges to its generalization ability. To address these issues, we introduced a smoothness regularization method and the Segment Deactivation technique, effectively enhancing KAN’s robustness by reducing overfitting to noise and promoting model smoothness.

References

- [1] Alexander Dylan Bodner, Antonio Santiago Tepsich, Jack Natan Spolski, and Santiago Pourteau. Convolutional kolmogorov-arnold networks. *arXiv preprint arXiv:2406.13155*, 2024. 1
- [2] Zavareh Bozorgasl and Hao Chen. Wav-kan: Wavelet kolmogorov-arnold networks. *arXiv preprint arXiv:2405.12832*, 2024.
- [3] Roman Bresson, Giannis Nikolentzos, George Panagopoulos, Michail Chatzianastasis, Jun Pang, and Michalis Vazirgiannis. Kagnns: Kolmogorov-arnold networks meet graph learning. *arXiv preprint arXiv:2406.18380*, 2024. 1
- [4] Nicolas Carion, Francisco Massa, Gabriel Synnaeve, Nicolas Usunier, Alexander Kirillov, and Sergey Zagoruyko. End-to-end object detection with transformers. In *European conference on computer vision*, pages 213–229. Springer, 2020. 1
- [5] Bowen Cheng, Alexander G Schwing, and Alexander Kirillov. Per-pixel classification is not all you need for semantic segmentation. In *Proceedings of the IEEE/CVF Conference on Computer Vision and Pattern Recognition (CVPR)*, 2021.
- [6] Alexey Dosovitskiy. An image is worth 16x16 words: Transformers for image recognition at scale. *arXiv preprint arXiv:2010.11929*, 2020. 1
- [7] Mark Everingham, Luc Van Gool, Christopher KI Williams, John Winn, and Andrew Zisserman. The pascal visual object classes (voc) challenge. In *International Journal of Computer Vision*, pages 303–338. Springer, 2010. 4
- [8] Remi Genet and Hugo Inzirillo. A temporal kolmogorov-arnold transformer for time series forecasting. *arXiv preprint arXiv:2406.02486*, 2024. 1
- [9] Simon Haykin. *Neural networks and learning machines*, 3/E. Pearson Education India, 2009. 1
- [10] Kaiming He, Xiangyu Zhang, Shaoqing Ren, and Jian Sun. Deep residual learning for image recognition. In *Proceedings of the IEEE Conference on Computer Vision and Pattern Recognition (CVPR)*, pages 770–778, 2016. 1
- [11] John J Hopfield. Neural networks and physical systems with emergent collective computational abilities. *Proceedings of the national academy of sciences*, 79(8):2554–2558, 1982. 1
- [12] Andrew G Howard. Mobilenets: Efficient convolutional neural networks for mobile vision applications. *arXiv preprint arXiv:1704.04861*, 2017. 4
- [13] Gao Huang, Zhuang Liu, Laurens Van Der Maaten, and Kilian Q Weinberger. Densely connected convolutional networks. In *Proceedings of the IEEE Conference on Computer Vision and Pattern Recognition (CVPR)*, pages 4700–4708, 2017. 1
- [14] A.N. Kolmogorov. On the representation of continuous functions of several variables as superpositions of continuous functions of a smaller number of variables. *Doklady Akademii Nauk SSSR*, 108(2):179–182, 1956. 1
- [15] Andrei Nikolaevich Kolmogorov. On the representation of continuous functions of many variables by superposition of

- continuous functions of one variable and addition. In *Doklady Akademii Nauk*, pages 953–956. Russian Academy of Sciences, 1957. 1
- [16] Alex Krizhevsky and Geoffrey Hinton. Learning multiple layers of features from tiny images. Technical report, University of Toronto, 2009. 4
- [17] Alex Krizhevsky, Ilya Sutskever, and Geoffrey E Hinton. Imagenet classification with deep convolutional neural networks. *Advances in neural information processing systems*, 25, 2012. 1
- [18] Yann LeCun, Bernhard Boser, John S Denker, Donnie Henderson, Richard E Howard, Wayne Hubbard, and Lawrence D Jackel. Backpropagation applied to handwritten zip code recognition. *Neural computation*, 1(4):541–551, 1989. 1
- [19] Yann LeCun, Yoshua Bengio, and Geoffrey Hinton. Deep learning. *nature*, 521(7553):436–444, 2015. 1
- [20] Ze Liu, Yutong Lin, Yue Cao, Han Hu, Yixuan Wei, Zheng Zhang, Stephen Lin, and Baining Guo. Swin transformer: Hierarchical vision transformer using shifted windows. In *Proceedings of the IEEE/CVF International Conference on Computer Vision (ICCV)*, pages 10012–10022, 2021. 1
- [21] Ziming Liu, Yixuan Wang, Sachin Vaidya, Fabian Ruehle, James Halverson, Marin Soljačić, Thomas Y Hou, and Max Tegmark. Kan: Kolmogorov-arnold networks. *arXiv preprint arXiv:2404.19756*, 2024. 1
- [22] Jonathan Long, Evan Shelhamer, and Trevor Darrell. Fully convolutional networks for semantic segmentation. In *Proceedings of the IEEE conference on computer vision and pattern recognition*, pages 3431–3440, 2015. 1
- [23] J Redmon. You only look once: Unified, real-time object detection. In *Proceedings of the IEEE conference on computer vision and pattern recognition*, 2016. 1
- [24] Olaf Ronneberger, Philipp Fischer, and Thomas Brox. U-net: Convolutional networks for biomedical image segmentation. In *Medical image computing and computer-assisted intervention—MICCAI 2015: 18th international conference, Munich, Germany, October 5-9, 2015, proceedings, part III 18*, pages 234–241. Springer, 2015. 4
- [25] David E Rumelhart, Geoffrey E Hinton, and Ronald J Williams. *Learning representations by back-propagating errors*. Macmillan Publishers Ltd., 1986. 3
- [26] Mark Sandler, Andrew Howard, Menglong Zhu, Andrey Zhmoginov, and Liang-Chieh Chen. Mobilenetv2: Inverted residuals and linear bottlenecks. In *Proceedings of the IEEE conference on computer vision and pattern recognition*, pages 4510–4520, 2018. 4
- [27] Isaac J Schoenberg. Contributions to the problem of approximation of equidistant data by analytic functions: Part a.—on the problem of smoothing or graduation. a first class of analytic approximation formulae. *IJ Schoenberg selected papers*, pages 3–57, 1988. 1
- [28] Karen Simonyan and Andrew Zisserman. Very deep convolutional networks for large-scale image recognition. In *Proceedings of the International Conference on Learning Representations (ICLR)*, 2015. 1
- [29] David A Sprecher and Sorin Draghici. Space-filling curves and kolmogorov superposition-based neural networks. *Neural Networks*, 15(1):57–67, 2002. 1
- [30] Nitish Srivastava, Geoffrey Hinton, Alex Krizhevsky, Ilya Sutskever, and Ruslan Salakhutdinov. Dropout: A simple way to prevent neural networks from overfitting. In *Journal of Machine Learning Research*, pages 1929–1958, 2014. 7
- [31] Robert Tibshirani. Regression shrinkage and selection via the lasso. *Journal of the Royal Statistical Society: Series B (Methodological)*, 58(1):267–288, 1996. 5
- [32] Cristian J Vaca-Rubio, Luis Blanco, Roberto Pereira, and Mărius Caus. Kolmogorov-arnold networks (kans) for time series analysis. *arXiv preprint arXiv:2405.08790*, 2024. 1
- [33] A Vaswani. Attention is all you need. *Advances in Neural Information Processing Systems*, 2017. 1
- [34] Wenhai Wang, Enze Xie, Xiang Li, Dengping Fan, Mingming Song, Ding Liang, Tong Lu, Ping Luo, and Ling Shao. Pyramid vision transformer: A versatile backbone for dense prediction without convolutions. In *Proceedings of the IEEE/CVF International Conference on Computer Vision (ICCV)*, pages 568–578, 2021.
- [35] Li Yuan, Yunpeng Chen, Tao Wang, Weihao Yu, Yingyan Shi, Zihang Jiang, Francis EH Tay, Jiashi Feng, and Shuicheng Yan. Tokens-to-token vit: Training vision transformers from scratch on imagenet. *arXiv preprint arXiv:2101.11986*, 2021. 1